Implementation of a Biometric Iris Recognition System for Person Identification

Miguel Colores¹, Mireya García¹, Alejandro Ramírez²,

¹ Instituto Politécnico Nacional-CITEDI, Av. Del Parque No.1310, Tijuana BC, colores, mgarciav@citedi.mx
² Dpto R&D, PILIMTEC, Châteaugiron, Francia alramirez 10@yahoo.fr

Abstract. Iris recognition has received increasing attention in recent years because their biometrics features can be used on security systems applications, due to their great advantages, such as variability, stability and security. This paper presents a description of a biometric system for person identification based on the iris pattern. For the system implementation some known techniques are proposed for the segmentation, encoding and pattern comparison stages of the recognition.

Keywords: Biometrics, coding, identification, iris pattern.

1 Introduction

Biometric identification technologies, including facial recognition, fingerprint recognition, speaker verification and others, offer a new solution for personal identification, because they offer a more natural way for performing identification [1][2]. Technologies that use biometrics features have a potential application identifying individuals in order to control access to secured areas or services. Nowadays a lot of biometric techniques are being developed based on different features and algorithms. Each technique has its advantages and limitations, and it's not possible to determine which is the best, without considering first the application environment. Nevertheless, it is well known that, from all of these techniques, iris recognition is one of the most promising for high security applications. The possibility that the iris (Fig. 1.a) can be used as a kind of optical fingerprint for person identification was first suggested by ophthalmologists. Automated systems for person identification based on iris recognition are considered to be the most reliable among all biometric methods; this because a biometric identification system making many comparisons between different patterns of persons can give false results, but the probability of finding two people with identical iris pattern is almost zero [3]. For this reason, iris recognition technology is becoming an

© A. Argüelles, J. L. Oropeza, O. Camacho, O. Espinosa (Eds.) Computer Engineering.

Research in Computing Science 30, 2007, pp. 47-56

important biometric solution for people identification in applications such as access control. Other applications include immigration controls using biometric passports [4].

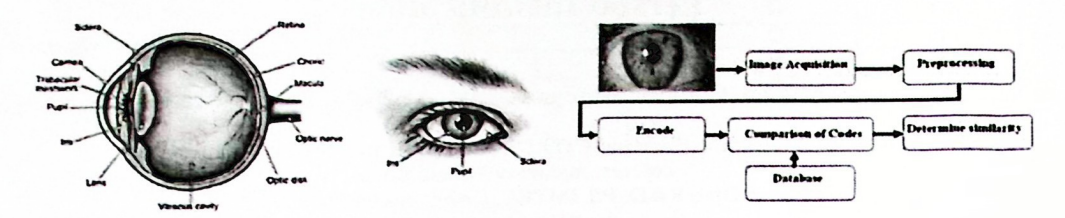


Fig. 1. a) Iris location: Lateral and frontal views. b) Iris Recognition System.

Only two iris recognition prototypes had been developed: one by J. Daugman [5], and the other by W. Wildes [6]. Most of the commercial iris recognition systems use the algorithms proposed by Daugman. One of the most successful commercial iris recognition systems is distributed by Iridian Technologies [7] and it uses algorithms patented by Daugman. That company has developed the entire recognition system (Fig. 1.b) which consists of the following steps: Firstly, an image of the user's eye is captured by the system (Images Acquisition). Then, the image is processed to normalize the scale and illumination of the iris. This region is localized and separated of the eye image (Preprocessing). Thirdly, features that represent the iris patterns are extracted and a code is generated (Encode). And finally, a decision is made by matching the code generated by the iris (comparison of codes and Determine Similarity).

The objective of this article is to present the implementation of an iris recognition system based in mathematical algorithms derived from the information found in open source literature. Since it is knows, the algorithms used in commercial system (Daugman's system) are not available. In this article the different concepts for every stage in an iris recognition system was developed by our-self implementing in C language in order to verify the system performance and to validate the chosen options for every stage. In section 2, we will introduce the iris acquisition device. Section 3 will discuss the preprocessing. Section 4 is about iris feature extraction. Section 5 will discuss the comparison of codes and how is made the decision when codes generates by iris are matching. The experiments and results will be presented in the section 6. Finally conclusions will be drawn in section 7.

2 Iris Image Acquisitions

This stage is important and difficult in an iris recognition system. Since iris is small in size and dark in color, is difficult to acquire good images for analysis using the standard CCD camera and ordinary lighting. It is necessary to use a special device for images acquisition which can deliver eyes image with sufficiently high quality while that remains as system noninvasive to the human operator. We need to considerate image acquisition

with sufficient resolution and sharpness to support recognition, good contrast without resorting to a level of illumination that annoys the operator, and the optical aberrations and reflections should be eliminated as much as possible. One schematic diagram for image acquisition well-known because fulfills the requirements, was develop by John Daugman (Fig. 2.a).

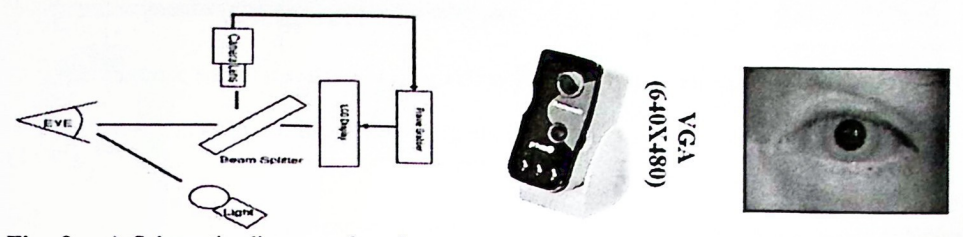


Fig. 2. a) Schematic diagram of an image acquisition system. b) Example of an iris image captured with a camera BMET100US.

The system don't use color information, use monochrome cameras with 8 bits gray-level resolution, because the color information provide additional discriminatory power. The positioning of the iris for image capture is concerned with framing the entire iris in the camera's field of view with good focus, so the system requires that the operator positions itself his eye region in front of the camera. For this reason the diagram provides a live video feedback via a miniature liquid crystal display placed in line with the camera's optics via a beam splitter. This allows the operator to see what the camera is capturing and to adjust his position accordingly [8]. In our experiments we work with a camera BMET100US of Panasonic (Fig. 2.b).

3 Preprocessing

An iris image contains some irrelevant parts (eg. eyelid, sclera, pupil, etc) (See Fig. 1.a). Even for the iris of the same eye, its size may vary depending on eye to camera distance as well as light brightness. Therefore, before matching the original image needs to be preprocessed to localize and normalize the iris.

3.1 Iris Localization

In this stage the iris is detected and isolated from the image, namely, finding both the inner (papillary) and the outer (sclera boundaries) (see Fig. 1.a). The captured image is a 2-D array and is described as I(x, y) where the point (x, y) is the gray-level. The first eye part to isolate is the pupil, knowing that the pupil region is generally darker than its surroundings (Fig. 3-c) that is used to fix a region threshold to binarize the image I(x, y) (Fig. 3-a) to obtain an image I(x, y) (Fig. 3-b), the image is scanning in the horizontal direction to find the longest chord which will be the diameter of the pupil.

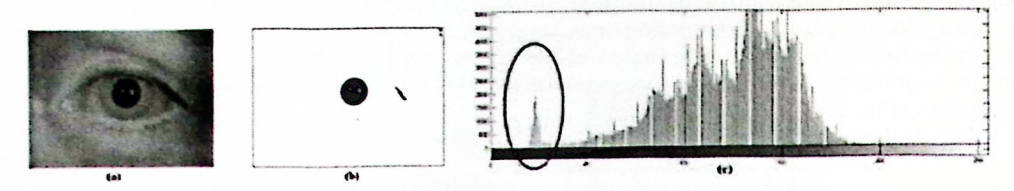


Fig. 3. (a) Original image I(x,y). (b)Binary image Ib(x,y) (c) Gray levels for the pupil region.

Thus the centroide coordinates of the pupil are gives by the followings equations:

$$x_p = x + \frac{D(x, y)}{2} \tag{2}$$

$$y_p = yy_p = y$$

$$r_p(ratio) = \frac{D(x, y)}{2} \tag{3}$$

Where D is the longest chord, and (x, y) is the start point of D.

The outer boundary of the iris is more difficult to detect because of the low contrast between the two sides of the boundary. Then Canny edge detection is performed to create an edge map to generate gradients information [9]. Circular Hough Transform which is employed by Wildes [10], is used to detecting the iris-sclera boundary to obtain a new centre (x_s,y_s) and radio r_s , also the linear Hough Transform [11] is used to detect and isolate eyelids and eyelashes.

3.2 Iris Normalization

Once the pupil and sclera boundaries are extracted and the iris ring is localized, the captured iris image which always varies in size is normalized into a rectangular block by a Cartesian to polar reference transform, suggested by J.Daugman [5]. In this way is compensate the stretching of the iris texture as the pupil changes in size, and is unfold the frequency information contained in the circular texture in order to facilitate next features extraction. Moreover, this new representation allows to separating the iris from the pupil. Thus the polar transform is implementing by the following mapping (Fig. 4)

$$I(x(\rho,\theta),y(\rho,\theta)) \to I(\rho,\theta)$$
 (4)

$$x(\rho,\theta) = (1-\rho)^* x_p(\theta) + \rho^* x_s(\theta)$$
 (5)

$$y(\rho,\theta) = (1-\rho) * y_p(\theta) + \rho * y_s(\theta)$$

The θ ($\theta \in [0;2\pi]$) and ρ ($\rho \in [0;1]$) parameters dimensionless describe the polar coordinate system. I(x,y) is the region image,(x,y) are the original Cartesian coordinates (r, θ) are the corresponding normalised polar coordinates, (x_p(θ),y_p(θ)) and (x_s(θ),y_s(θ)) are the coordinates of the iris ring along the θ direction.

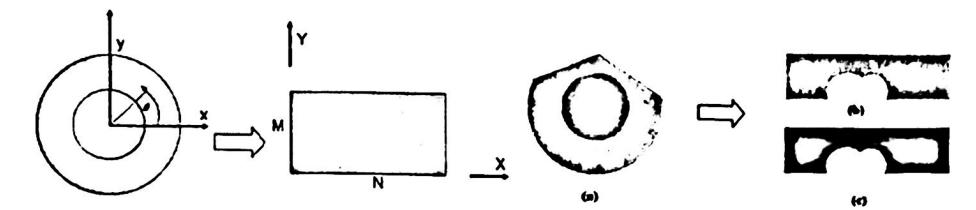


Fig. 4. Iris rectangular representation. a) Iris localization on an eye image. b) Iris mask. c) Noise mask.

Besides to generate the normalized iris image (Fig. 4.b) "iris mask" is necessary to generate another image called "noise mask" (Fig. 4.c). This mask indicates the regions of the normalized iris where the pattern of the iris is obstructed by the eyelids, eyelashes, etc. The noise mask has the same dimensions that the iris mask, its used in the comparison stage to avoid compares the obstructed regions.

4 Iris feature encode

This stage is to extract the information of the iris pattern and needed to be encoded for matching purposes. The iris features are obtained convolving the normalized iris pattern with a 1D Log-Gabor filters. Gabor Filters based methods have been widely used as feature extractor in computer vision, especially for texture analysis [12]. Daugman [5, 13] used multi-scale Gabor wavelets to extract phase structure information of the iris texture. However, Field [14] has examined that there is a disadvantage of the Gabor Filter in which the even symmetric filter will have a DC component whenever the bandwidth is larger than one octave. To overcome this disadvantage, another type of filter is used known as Log-Gabor, which is Gaussian on a logarithmic scale, can be used to produce zero DC components for any bandwidth. The Log-Gabor filters are obtained by multiplying the radial and angular components together where each even and odd symmetric pair of Log-Gabor filters comprises a complex Log-Gabor filter at one scale. The frequency response of a Log-Gabor Filters is given as:

$$G(f) = e^{\frac{-(\log(f/f_0))^2}{2(\log(\beta/f_0))^2}}$$
(7)

Where f_0 represents the central frequency, and β bandwidth of the filters.

For the implementation of 1D Log-Gabor Filter is chosen to be the feature extractor of iris since 1D Log-Gabor Filters is an improved version of Gabor Filters. By applying 1D

Log-Gabor Filters, 2D normalized pattern is divided into a number of 1D signals, and these 1D signals are convolved with 1D Gabor wavelet. The rows of the 2D normalized pattern are taken as the 1D signal; each row corresponds to a circular ring on the iris region. The angular direction is taken rather than the radial one, which corresponds to columns of the normalized pattern, since maximum independence occurs in the angular direction. The row of the image is X = [P(1), P(2), ..., P(N)]. First is applied a discrete Fourier transform (DFT) on the vector X to get vector Y (eq.8). Then multiply vector Y and a 1-D log-Gabor wavelet to get the vector Z (eq.9). The 1D Log-Gabor function is defined (eq.7), only one filter is used, with $f_0 = 12$, and a bandwidth $\beta = 0.5$ [15]. Finally, using the inverse DFT on the vector Z to get the vector D (eq.10).

$$Y_{k} = \sum_{n=1}^{N} x_{n} e^{-j2\pi(k-1)(n-1)/N}$$

$$z_{k} = Y_{k} \times G_{k}$$
(8)

$$z_{k} = Y_{k} \times G_{k} \tag{9}$$

$$D_{k} = \frac{1}{N} \sum_{n=1}^{N} z_{k} e^{-j2\pi(k-1)(n-1)/N}$$
 (10)

The output h of the Gabor filter is complex numbers h=h_{Re}+h_{lm}, where the phase angle at each output point is quantized to two bits depending on the quadrant where this each element in the complex plane (Fig. 5). Thus for an image normalized with size (MxN) the resulting template is of size (Mx2N). The template size with radial resolution of 128 pixels and angular resolution of 256 pixels was chosen. These parameters generate an iris template that contains 32768 bits of information.

5 Comparison of codes

For this process is used the Hamming distance (HD) that gives a measure of how many bits are the same between two bit patterns. Using the Hamming distance of two bit patterns, a decision can be made as to whether the two patterns were generated from different irises or from the same one. Since an individual iris region contains many features, each iris region will produce a bit-pattern which is independent to that produced by another iris, and two iris codes produced from the same iris will be highly correlated. If two bits patterns are completely independent, such as iris templates generated from different irises, the Hamming distance between the two patterns should equal 0.5. This occurs because independence implies the two bit patterns will be totally random, so there is 0.5 chance of setting any bit to 1, and vice versa. Therefore, half of the bits will agree and half will disagree between the two patterns. If two patterns are derived from the same iris, the Hamming distance between them will be close to 0.0, since they are highly correlated and the bits should agree between the two iris codes. For matching, the Hamming distance was chosen as a metric for recognition, since bit-wise comparisons were necessary. The Hamming distance algorithm employed also incorporates noise masking, so that only significant bits are used in calculating the Hamming distance between two iris templates (A,B).

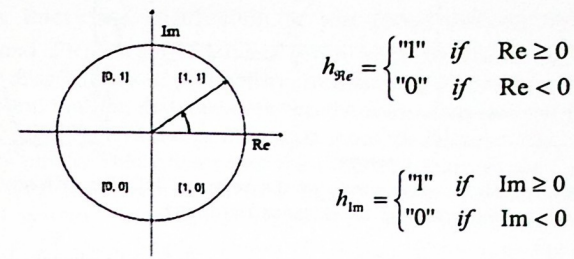


Fig. 5. How is quantize in 2 bits the filter output

Both iris patterns (maskA,maskB) are used in the calculation. The Hamming distance will be calculated using only the bits generated from the true iris region given by the equation:

$$HD(A,B) = \frac{1}{\sum_{i,j} C(i,j)} \sum_{i,j} (A(i,j) \text{ xor } B(i,j) \& C(i,j)$$
 (11)

where

$$C(i,j) = \begin{cases} 1 & \text{if } maskA(i,j) = 0 \\ 0 & \text{otherwise} \end{cases}$$
 (12)

Although, in theory, two iris templates generated from the same iris will have a Hamming distance of 0.0, in practice this will not occur. Normalization is not perfect, and also there will be some noise that goes undetected, so some variation will be present when comparing two intra-class iris templates. In order to account for rotational inconsistencies, when the Hamming distance of two templates is calculated, one template is shifted left and right bit-wise and a number of Hamming distance values are calculated from successive shifts. This bit-wise shifting in the horizontal direction corresponds to rotation of the original iris region by an angle given by the angular resolution used. To calculate HD between A and B, we fix the code A, and shift the code B from -15° to +15° with an increment of 1.5°. The minimum HD from these shift positions is used as the reported HD. The recognition is based on a test of statistical independence obtained comparing iris patterns (binary codes) generated by same and different eyes [16]. In the figure 6.a the curve "Intra-class" shows the HD between two iris templates generated by one eye, and the curve "Inter-class" shows the HD between the iris templates generated by different eyes, as a function of the rotation amount applied. The fig. 6.b shows a typical curves of probability distribution of the distance Hamming. (Intra-class) generated by comparing patterns generated by the same eye and (Inter-class) comparing patterns generated by comparing patterns by different eyes.

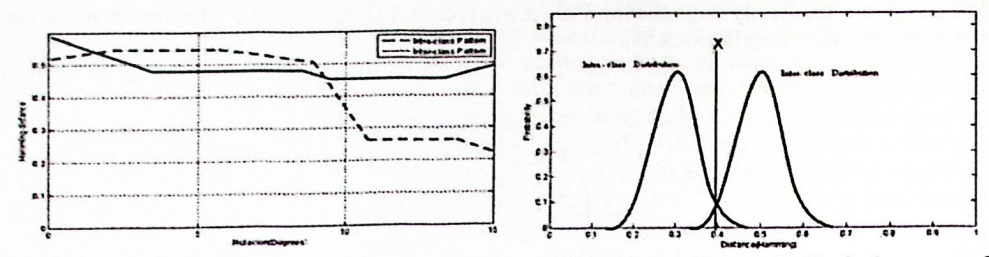


Fig. 6. a) Show an example of the reported HD for different rotations. b) Typical curves of probability distribution of the distance Hamming.

To make a recognition decision can be defined a threshold X. If the obtained distance of Hamming is minor who thresholds X, is decided that the compared codes were generated by same eye, otherwise is decided that they were generated by different eyes. Both distributions Inter-class and intra-class, generally, are overlapped. For that reason, the area under the distribution Inter-class to the left of threshold X, represents the probability of a false identification, whereas the area under the distribution intra-class to the right of threshold X, represents the probability of a false rejection. These measures are known as false acceptance rate (FAR) and false rejection rate (FRR). The distance for both distributions ("decidability") can be calculate by equation (13), this value can be used to optimize the parameters on log-Gabor filters

$$d = \frac{|\mu_I - \mu_D|}{\sqrt{{\sigma_I}^2 + {\sigma_D}^2/2}}$$
 (13)

where

 μ_I , μ_D = the mean of the probabilit y distributi ons

 σ_I , σ_D = standard deviation of the probabilit y distributions

6 Results

This section describes the experiments using an iris image database "CASIA" [17] for evaluating matching performance and the effectiveness of the algorithms. This database contains images of 20 different irises and every iris has 3 images with 320 × 280 pixels in 256 gray levels. The experiments were obtained with verifications (one to one matching). Firstly, evaluating genuine matching scores for all the possible combinations (60 intraclass comparisons). Then evaluating the impostor matching scores for all the possible combinations (190 inter-class comparisons). There are a number of parameters required in processing feature extraction using Log-Gabor Filters. Optimum settings for these parameters are needed to attain the best verification rate. To select an optimal Log-Gabor filter parameters we probe different values, obtaining that features for iris can be extracted with bandwidth \square = 0.5, one with center wavelength fo=14 pixels. In a second stage of

experimentation, the values for the False Acceptance Rate (FAR) and the False Reject Rate (FRR) was estimate. Both distributions obtained were adjusted to a normal distribution with parameters $\mu_I = .182$ $\sigma_I = .029$ for Intra-class distribution and $\mu_D = .4195$ $\sigma_D = .0534$ for Inter-class Distribution. It was found that the optimal values for (FAR=.182516% and FRR=.185026%) are given with threshold fixed in X=.2645. The Fig. 7 shows the distributions of probability for matching distance for intraclass and inter-class. It was found that the distance between the intra-class and the interclass distribution is large (d=5.52732), and the portion that overlaps between the intraclass and the inter-class is very small. This proves that the proposed features are highly discriminating. In addition, several tests were made to obtain the time of execution for each stage in the implemented system: Binarization (time:71.8 ms), Pupil Localization (135.2 ms), Iris Localization (362.8 ms), Normalization (64.2 ms), Extraction Features (12.65 ms), Iris Code Extraction (15.07 ms), Iris Code Matching (131.7 ms), Total: 793.42 ms. The time computation consumed by each stage of the system that was implemented on a P4 computer (1.8 GHz, 512 MB RAM, Windows XP). The average total execution time of a basic verification process not exceeds 800 ms, which is suitable for a recognition system.

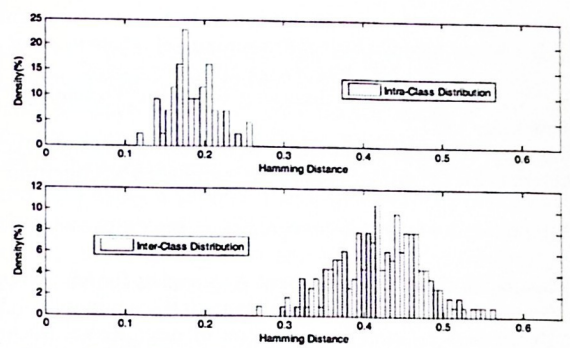


Fig. 7. Distributions of probability intra-class and inter-class in function to hamming distance.

This kind of information is not reported commonly in the literature. Therefore a comparison between the obtained results and another system cannot be done. This is to the lack of public datasets. It is highlighted that the algorithms operations were programmed with double precision floating-point to obtain greater exactitude in the results.

7 CONCLUSIONS

The objective of this article was to present the implementation of an iris recognition system based in mathematical algorithms derived from the information found in open source literature. Different concepts for every stage in a iris recognition system was

developed by our-self implementing in C language in order to verify the system performance and to validate the chosen options for every stage. The selection of the parameters and the algorithms for every stage has been adopted to ensure the system maintains a good compromise between accuracy and speed. The evaluation of the system achieved high confidence identity verification based on iris texture; further efforts should be applied to be insensitive to variations in the conditions of iris images acquisition.

References

[1] Kresimir Delac, Mislav Grgic ."A survey of Biometric Recognition Methods " 46th International Symposium Electronics in Marine, ELMAR-2004, 16-18 June 2004, Zadar, Croatia.

[2] R.Garcia, C.Lopez, O.Aghzout, J.ruiz, "biometric Identification Systems" Signal Processing,

V.83 n.12 December 2003.

[3] Y.Belganoui, J.C Guézel and T. Mahé, "La biométrie, sesame absolu...", Indistries et Techniques, france, no 817, July 2000.

[4] "Iris recognition border-crossing system in the UAE". Reproduced from International Airport

Review, Issue 2, 2004.

- [5] John Daugman, "High confidence visual recognition of persons by a test of statical independence" ,IEEE Transactions On Pattern analysis and Machine Intelligence,vol.15,no 11 November 1993.
- [6] W.W.Boles and B.Boashash, "a human identification technique using images of the iris and wavelet transform", IEEE Transactions On Signal Processing, vol. 45, no 4, April 1998.

[7 Iridian Technologies, "Moorestown, NJ". http://www.iridiantech.com/

- [8] Richard P. Wildes, "Iris recognition: An Emerging Biometric Technology" Proceedings of the IEEE, vol. 85,no. 9, september 1997.
- [9] J.F.Canny, "Finding edges and lines in images" M.S. thesis ,Mass.Inst .Technologies,1983. [10] R.P.Wildes, J.C.Asmuth, G.L.Green "A System for Automated Recognition" 0-8186-6410-X/94
- JEEE 1994. [11] P.V.C.Hough, "Method and means for recognizing complex patterns". U.S. Patent 3 069 654,1962.
- [12] Sánchez Avila, C Sánchez Reíllo "Two Different Approaches for Iris Recognition using Gabor Filters and Multiscale Zero-Crossing Representación" Pattern Recognition Vol:38 nº ,23 July 2004.
- [13] John Daugman, "Uncertainly relation for resolution in space, spatial frecuency, ans orientation optimized by two dimensional visual cortical filters," J Opt.Soc.Amer .A. ,vol.2.,pp.1160-1169,1985.
- [14] D Field ."Relations between the statics of natural images and the response propierties of cortical cells" Journal of the Optical Society of America, 1987.
- [15] Chong S, Andrew T, David N, "High security Iris verification system based on random secret integration" Computer Vision and Image Understanding, Vol 102, Issue 2, May2006, Pag.169-177. [16] W.P. Tanner & J.a. Swets,"A desicion-making theory of visual detection,"Psychol.rev.vol 61 pp. 401-409, 1954.

[17] "CASIA" iris image database collected by institute of automation, Chinese academy of

sciences. Available: www.sinobiometrics.com.